Atomic Size Effects in Pressure-Induced Amorphization of a Binary Covalent Lattice

Meijie Tang and Sidney Yip

Department of Nuclear Engineering, Massachusetts Institute of Technology, Cambridge, Massachusetts 02139-4307

Applying a bond-order potential model to describe a binary covalent solid (SiC) in a molecular dynamics simulation, we show that under hydrostatic compression the homogeneous lattice undergoes an amorphous transition triggered by an elastic shear instability, with the critical pressure agreeing well with that determined from finite-load stability criteria. By modifying the potential model to suppress either atomic size difference or mixed bond preference, we demonstrate that the former effect can be dominant in favoring amorphization over polymorphic transition.

When a crystal lattice becomes structurally unstable under pressure, two types of responses generally can be expected, a polymorphic transformation to another structure or a transition to a disordered state, the latter being a particular case of the phenomenon of solid-state amorphization. From the standpoint of phase stability of stressed solids, it is clearly of fundamental interest to be able to predict, for a given solid, the critical pressure at which the instability occurs, and understand what factors govern the "deformation" path the system will follow.

Conventional theoretical analysis of the polymorphic transition between two structures tends to involve a determination of the cohesive energy curves from which the critical pressure is obtained by a common tangent construction [1]. However, such an approach generally does not take into account the possible existence of an activation barrier separating the two structural phases. Recently, it has been shown that for homogeneous lattices, elastic stability criteria, expressed in terms of current-state elastic constants and the applied stress, provide a practical means of determining not only the critical condition of stress or strain, but also the nature of the triggering instability [2]. Thus, one has an alternative approach, one based on mechanical response, to the analysis of stability of solids at finite loading.

In this Letter we report a study of the crystal-to-amorphous transition in a homogeneous binary covalent lattice using a model interatomic potential developed to describe β-SiC. We show that the critical pressure at which the transition is observed in a molecular dynamics simulation is that predicted by the aforementioned stability criteria, and that the instability is caused by the vanishing of the shear modulus, itself a consequence of internal strain relaxation. Moreover, we compare the stability analysis of the binary lattice using the model of SiC with that of an elemental lattice using a similar model for Si, the latter having been shown recently to undergo a polymorphic transition under pressure (diamond cubic to β-Sn). We demonstrate that disordering of the binary lattice arises from the effects of atomic size difference, which are obviously absent in an elemental lattice. These

results, made possible by manipulating the potential model describing SiC [3] to suppress either size effect or chemical bond preference, point to a subtle competition between two shear instabilities, the vanishing of the rhombohedral shear modulus leading to amorphization in the SiC model, on the one hand, and the vanishing of the tetragonal shear modulus leading to polymorphic transition in the Si model on the other hand. With regard to possible experimental correspondence, our findings appear to correspond to the recent observation of pressure-induced amorphization of a similar binary covalent compound, BAs [4]. While measurements on β-SiC which show amorphization under electron irradiation [5] and polymorphic transition under pressure [6] have been reported, as we discuss below, it would not be appropriate to attempt a direct comparison of the present results with data.

The empirical interatomic potential we have adopted to simulate a binary covalent solid is a modification of that developed by Tersoff [3] to model β-SiC. This is a many-body potential in which the local tetrahedral environment is treated through a bond order parameter b_{ij}. For the interaction between atoms i and j, b_{ij} also depends on other neighboring atoms; as a result the interaction of a Si with its C neighbor is not the same as that of a C with its Si neighbor. Our modification consists of scaling the interaction range cutoff with the lattice parameter [7] which among other benefits has the effect of avoiding the strong unphysical repulsion between second nearest neighbors which otherwise would occur suddenly under high compression. The resulting cohesive energy curve is found to be in excellent agreement with *ab initio* results throughout the entire range of compression in this study, as well as a considerable range of volume change in tension. A molecular dynamics simulation is carried out in a cell of 216 atoms, arranged in the zinc-blende structure at an initial lattice parameter $a_0 = 4.326$ Å, with periodic boundary conditions. Hydrostatic pressure is applied via the method of Parrinello and Rahman [8] which allows the simulation cell to respond by volume and shape changes. The equations of motion are integrated by means of a predictor-corrector

algorithm with a time step size of 4.8×10^{-5} ps. At each applied loading, the system is allowed to reach equilibrium in 60 000 time steps, after which another 60 000 steps are taken to collect trajectory data for property calculations. The simulation begins at zero pressure; at each incremental load increase, the atomic configuration obtained at the end of the preceding load is used as an initial configuration for the succeeding load. All runs are made at a temperature of 300 K, maintained by velocity rescaling at every time step.

The overall system response to pressure loading is shown in Fig. 1. As compression proceeds one sees initially normal behavior of volume decrease and potential energy increase, along with a near constant static structure factor $s(\mathbf{k})$, evaluated for $\mathbf{k} = (2\pi/a)(1,1,1)$. This behavior continues until an abrupt change occurs at $P = 707$ GPa. Referring to the system states just before and after the change as A and B, respectively, we find that in going from A to B by a small increment in the applied pressure, $s(\mathbf{k})$ drops sharply to an essentially zero value. Correspondingly, the system volume shows a slight increase [note the enlarged scale in Fig. 1(c)], while the potential energy decreases. Direct inspection of the instantaneous atomic configurations at these two states confirms that the lattice has gone from a perfectly ordered state at A to a fully disordered state at B. We therefore interpret the observed process as a crystal-to-amorphous transition induced by compression.

Figure 2 shows that the temporal variations of $s(\mathbf{k})$, V, and E_p indeed occur in concert and extend over a period

FIG. 2. Time-dependent responses at state B (a) $s(\mathbf{k})$, (b) volume, (c) energy per atom, and (d) off-diagonal elements of the cell matrix h (in units of 1.87 Å).
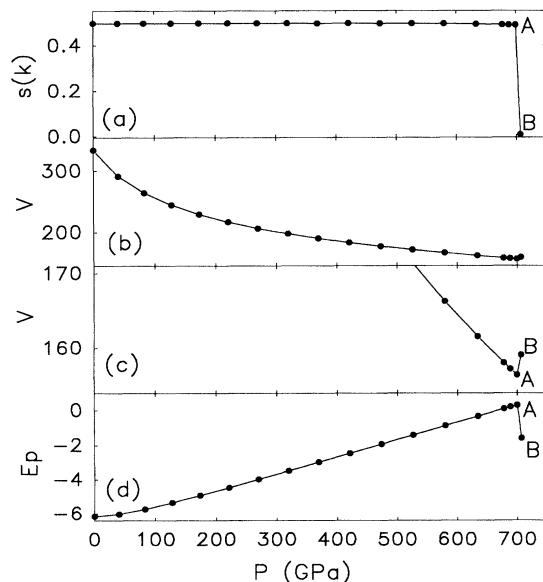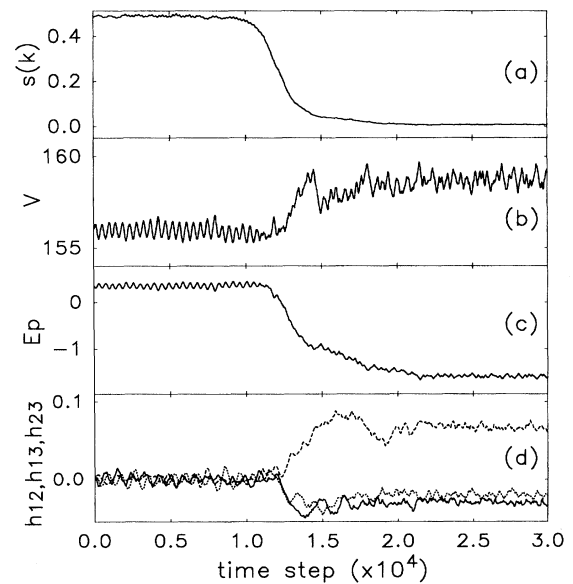

FIG. 1. System responses to compression (a) static structure factor, (b) simulation cell volume (in units of 6.538 Å^3), (c) same as (b) but on an expanded scale, and (d) internal energy per atom (in units of eV). P is time-averaged internal pressure.

of about 0.5 ps. While it is not surprising that both system volume and energy should show changes that reflect the loss of structural order, the fact that under such high pressure the system volume would increase and energy decrease may seem unusual. We have determined that, as a result of the structural rearrangement, the repulsive part of the energy decreased more than the increase in the attractive part, thus energy decreased as a whole. Here we note that in a previous molecular dynamics simulation of pressure-induced amorphization in α-quartz [9] an energy decrease also occurred at the transition. From the present results on the radial distribution functions, which clearly indicated that only short-range ordering remains at state B, we find that the collapse of the ordered lattice has allowed the Si-Si and C-C second nearest neighbors to move closer toward each other. Although every atom is still fourfold coordinated, the distributions of the tetrahedral angles and the cohesive energies of an atom have greatly changed. The angular distribution, previously sharply peaked about the characteristic 109.47°, becomes a practically uniform distribution over a range approximately from 70° to 130°. For the cohesive energy distribution per atom, both C and Si show a decrease in peak and average values, the changes being relatively more significant for C. It is conceivable that the detailed behavior of the energy and volume change upon amorphization can depend on quite subtle features of the potential model.

In Fig. 2 we show also the behavior of the off-diagonal components of the matrix h formed by the basis vectors of the simulation cell. In the Parrinello-Rahman method all nine components of h are allowed to vary during the simulation. When the off-diagonal elements become

nonzero, it means that the atomic configuration is undergoing a shear deformation. Thus Fig. 2(d) constitutes evidence that the abrupt system response is associated with a shear instability.

In view of the simulation results one may ask whether the observed critical pressure can be predicted by an appropriate stability analysis. For this purpose it is necessary to apply stability criteria [2] which take into account the effects of an applied load. In the present case, the criteria are $K(P) = (C_{11} + 2C_{12} + P)/3 > 0$, $G'(P) = (C_{11} - C_{12})/2 - P > 0$, $G(P) = C_{44} - P > 0$, where $K(P)$, $G'(P)$, and $G(P)$ may be regarded as the pressure-dependent bulk modulus, tetragonal and rhombohedral shear moduli, respectively, and C_{ij} are the isothermal elastic constants at the current state of stress [10]. We have calculated these moduli over the range of hydrostatic loadings where the zinc-blende lattice is predicted to be unstable. Figure 3(a) shows that as the lattice is compressed all moduli increase initially; however, under high compression $G(P)$ begins to decrease sharply, vanishes at $r/r_0 = 0.734$, corresponding to a pressure of 1156 GPa. At 300 K, $G(P)$ is found to vanish at $r/r_0 = 0.775$ corresponding to a pressure of 714 GPa, a prediction which is in satisfactory agreement with the critical pressure of 707 GPa directly observed in the simulation described above. Inspection of the individual components of C_{44} shows that the decrease of $G(P)$ arises from the abrupt enhancement of fluctuations in the shear stresses. Since this is a negative contribution, the accelerated change is responsible for the reversal in the pressure variation of $G(P)$, previously dominated by the monotonically increasing contribution to C_{44} from the Born term [10]. Physically, the effect causing the decrease in $G(P)$

FIG. 3. Variations of elastic moduli (in units of Mbar) with hydrostatic pressure in SiC (a) and Si (b) at 0 K, r and r_0 denote lattice parameters at current and zero pressure, respectively. Small circles denote the triggering instability for hydrostatic compression and tension.

can be attributed to internal strain relaxations [11] brought about by the increased pressure.

At this point it is useful to recall similar stability analysis results which have been obtained using the Tersoff potential with parameters determined for elemental Si [12]. As shown in Fig. 3(b), for Si in the diamond structure both $G(P)$ and $G'(P)$ decrease under sufficient compression, with $G'(P)$ vanishing first at $r/r_0 = 0.86$ and a corresponding pressure of 111 GPa. Since this tetragonal shear instability results in a transition from diamond cubic to β-Sn structure [12], one may ask, in view of Figs. 3(a) and 3(b), what is the origin of the different structural response to compression between the binary and elemental lattices. To address this question we consider the two fundamental effects associated with the binary nature of the SiC model, a difference in the atomic sizes of C and Si, and the chemical preference of Si (C) to have the other species as its nearest neighbors. Recently Tersoff has shown that size effect plays a much more dominant role in chemical ordering when the system is in its crystalline state than when it is in an amorphous state [13].

To separate the effects of size disparity from that of mixed bond preference, we note that the Tersoff potential is of the form $V_{ij} = f_c(r_{ij}) [A_{ij} e^{-\lambda_{ij} r_{ij}} - B_{ij} \chi b_{ij}] \times e^{-\mu_{ij} r_{ij}}$, where the two effects are described through the bond order parameter b_{ij} and the factor χ, respectively. (For definitions of the various quantities in this potential, readers should see Ref. [3].) Since $\chi = 1$ when i and j refer to atoms of the same species, its value affects only V_{s_i-c} and V_{c-s_i}, and therefore the heat of formation ΔH. On the other hand, to suppress the effect of atomic size difference, one can simply set $b_{c-j} = b_{s_i-j}$ in functional form. This observation leads us to examine two idealizations of the Tersoff potential, one in which mixed bond preference is suppressed through adjusting χ to give $\Delta H = 0$ (model I), and another in which size difference is suppressed by the method just described while at the same time adjusting χ so that ΔH remains unchanged (model II). By deriving an effective pair interaction from the many-body Tersoff potential one can see the physical meaning of model II, namely, it is the limiting case of the bond order potential when both species have the same atomic size. In Table I the elastic constants, lattice parameter, and cohesive energy calculated for the two idealized models at equilibrium configuration and 0 K are compared with values for the full model. It is clearly seen that while the elimination of chemical bond preference has little effect, all three elastic constants are significantly altered in the absence of atomic size difference. Although both $C_{11} - C_{12}$ and C_{44} are appreciably reduced, the lowering of the former is more drastic such that in model II the elastic instability is found to be the vanishing of G'. This result is consistent with the behavior obtained in the case of an elemental covalent lattice [12]. Thus we have shown that the difference between binary and elemental lattices
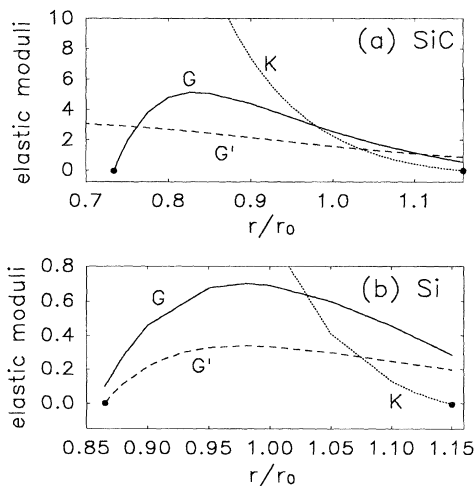
TABLE I. Comparison of properties calculated using the Tersoff potential and the two idealizations, models I and II.

	Tersoff	Model I	Model II
Lattice parameter (Å)	4.32	4.34	4.32
Cohesive energy (eV)	−6.19	−6.03	−6.19
Bulk modulus (Mbar)	2.25	2.18	2.25
C_{11} (Mbar)	4.36	4.19	3.31
C_{12}	1.20	1.17	1.72
C_{44}	2.56	2.42	1.61
$C_{11} - C_{12}$	3.16	3.02	1.59

in compression-induced structural response lies in the dominant role of atomic size effect. In other words, amorphization occurs in the SiC model because the onset of vanishing of G precludes a polymorphic transition associated with the instability of $G' = 0$. To demonstrate that this is the correct interpretation, we have carried out a simulation of model II under compression and indeed observed a transition from zinc blende to rock salt structure which is triggered by the tetragonal shear instability.

Experimentally, β-SiC has been observed to amorphize under electron irradiation [5], whereas under compression it transforms from zinc blende to rock salt structure at 100 GPa [6], a transition which was predicted at 60 GPa by first-principles calculation of cohesive energy [14]. A comparison of the present results, obtained for the homogeneous lattice, with measurements on samples which are not perfect crystals can be misleading unless the effects of inhomogeneities such as grain boundaries and other crystal defects can be assessed. We are also mindful that the validity of our results is restricted to that of the Tersoff potential model, the accuracy of which can be tested, so far as electronic structure effects are concerned, by simulations using the *ab initio* method or the tight-binding approximation. For example, the volume and energy changes upon amorphization discussed previously could be verified by these more rigorous methods. Even here it is good to note that a recent observation of amorphization of a similar covalent *AB* compound (BAs) at 125 GPa [4] was interpreted as a kinetically frustrated process; in this case first-principles calculation had predicted a polymorphic transition at about 110 GPa.

The present work is the first direct simulation of pressure-induced amorphization in which the unstable structural responses are unambiguously interpreted in terms of a specific elastic instability. While the phenomenon has been observed in a previous simulation of α-SiO$_2$ [9], the results were not analyzed in identifying the amorphization mechanism as a shear instability [15]. Since solid-state amorphization can be brought about by physically very different driving forces, ion and electron irradiations, chemical diffusion, and mechanical deformation [16], it has been conjectured whether hydrostatic pressure alone in a homogeneous lattice is sufficient to cause amorphization [17]. Present results and those on

α-SiO$_2$ [9] give an affirmative answer for the case of binary lattices. In particular, we have emphasized here the essential role of atomic size disparity for amorphization.

Our study also gives validity to the suggestion [17] that solid-state amorphization and melting are analogous phenomena in which one can distinguish heterogeneous and homogeneous processes of thermodynamic and mechanical nature, respectively. It has been shown that, in isobaric ($P = 0$) heating of a homogeneous lattice, the system can be superheated to a temperature where a tetragonal shear instability triggers a sequence of shear and dilatational deformation, resulting in a disordered state with all the signatures of a first-order transition [2]. In analogy to this thermoelastic process which one may call *mechanical melting*, the pressure-induced process studied here may be regarded as *mechanical amorphization*. Both are upper limits of metastability, homogeneous in nature, driven by an elastic instability, and observable only because the heterogeneous process has been suppressed.

[1] See, for example, M. T. Yin and M. L. Cohen, Phys. Rev. Lett. **45**, 1004 (1980); **26**, 5668 (1982).
[2] J. Wang, S. Yip, S. R. Phillpot, and D. W. Wolf, Phys. Rev. Lett. **74**, 4182 (1993); J. Wang, J. Li, S. Yip, S. R. Phillpot, and D. Wolf, Phys. Rev. B (to be published).
[3] J. Tersoff, Phys. Rev. B **39**, 5566 (1989).
[4] R. G. Greene, H. Luo, A. L. Ruoff, S. S. Trail, and F. J. DiSalvo, Phys. Rev. Lett. **73**, 2476 (1994).
[5] H. Inui, H. Mori, A. Suzuki, and H. Fujita, Philos. Mag. B **65**, 1 (1992).
[6] M. Yoshida, A. Onodera, M. Ueno, K. Takemura, and O. Shimomura, Phys. Rev. B **48**, 10 587 (1993).
[7] M. Tang, Ph.D. thesis, MIT, 1995; M. Tang and S. Yip, J. Appl. Phys. **76**, 2719 (1994).
[8] M. Parrinello and A. Rahman, J. Appl. Phys. **52**, 7182 (1981).
[9] J. S. Tse and D. D. Klug, Phys. Rev. Lett. **67**, 3559 (1991).
[10] J. R. Ray, Comput. Phys. Rep. **8**, 109 (1988).
[11] C. S. G. Cousins, J. Phys. C **11**, 4867, 4881 (1978).
[12] K. Mizushima, S. Yip, and E. Kaxiras, Phys. Rev. B **50**, 14 952 (1994).
[13] J. Tersoff, Phys. Rev. B **49**, 16 349 (1994).
[14] K. J. Chang and M. L. Cohen, Phys. Rev. B **35**, 8196 (1987).
[15] N. Binggeli and J. R. Chelikowsky, Phys. Rev. Lett. **69**, 2220 (1992).
[16] P. R. Okamoto and M. Meshii, in *Science of Advanced Materials,* edited by H. Wiedersich and M. Meshii (ASM International, Materials Park, 1990), p. 33.
[17] D. Wolf, P. R. Okamoto, S. Yip, J. F. Lutsko, and D. Kluge, J. Mater. Res. **5**, 286 (1990).